Inorg. Chem. **2006**, *45*, 2610–2618

Stabilization of Coordinated Carbonate in Aqueous Acidic Solution: Steric Inhibition of Protonation in Co(III) Complexes Containing Chelated Carbonate†

Sarah E. Cheyne, Lisa F. McClintock, and Allan G. Blackman*

Department of Chemistry, University of Otago, P.O. Box 56, Dunedin, New Zealand

Received December 13, 2005

The synthesis, characterization, X-ray crystal structures, and reactivity in aqueous acidic solution of the Co(III) carbonate complexes $[Co(tpa)(O_2CO)]ClO_4 \cdot H_2O$, $[Co(Me\text{-}tpa)(O_2CO)]ClO_4 \cdot 0.5H_2O$, $[Co(Me_2\text{-}tpa)(O_2CO)]ClO_4 \cdot 0.5H_2O$, and $[Co(Me_3\text{-}tpa)(O_2CO)]ClO_4$ are reported (tpa = tris(2-pyridylmethyl)amine; Me-tpa, Me_2-tpa, and Me_3-tpa are derivatives of tpa containing one, two, and three 6-methylpyridyl rings, respectively). The complexes display very different spectroscopic and ^{59}Co NMR properties, consistent with the decreasing ligand field strength of the tripodal amine ligands in the order tpa > Me-tpa > Me_2-tpa > Me_3-tpa. X-ray structural data show an increase in the average Co–N bond distances as the number of methyl groups on the tripodal amine ligand increases, and this is the result of steric interactions between the methyl groups and the carbonate ligand and between the methyl groups themselves. Rate data for the acid hydrolysis of $[Co(tpa)(O_2CO)]^+$ (I = 1.0 M ($NaClO_4$), 25.0 °C) over the $[HClO_4]$ range of 0.10–1.0 M are consistent with a previously proposed mechanism involving protonation of the carbonate ligand prior to ring-opening, but the equilibrium constant for protonation is smaller in this case than those obtained previously, as is the equilibrium constant for proton transfer from the exo to the endo O atoms. Comparative rate data ([HCl] = 6.0 M, 25.0 °C) for the four complexes show that those containing methylated ligands undergo acid hydrolysis between 25 and 90 times more slowly than $[Co(tpa)(O_2CO)]^+$ under the same conditions, and it is proposed that this rate difference is a result of steric factors. Inspection of space-filling diagrams shows that one of the endo oxygen atoms is significantly sterically hindered by the methyl groups of the tripodal amine ligands, thus inhibiting protonation at this site and leading to slower observed rates of hydrolysis. The results obtained in this study are consistent with the endo oxygen atoms being the mechanistically important site of protonation in the acid hydrolysis of metal complexes containing chelated carbonate.

Introduction

The acid hydrolysis of metal-coordinated carbonate provides one of the best examples of the change in reactivity that can occur on coordination of a ligand to a metal ion. Dissolution of simple soluble carbonate salts in acidic aqueous solution leads to rapid evolution of CO_2 through the intermediacy of H_2CO_3, with the rate constant for the $H_2CO_3 \rightarrow H_2O + CO_2$ reaction being on the order of 15−30 s^{-1},[1] and even nominally insoluble metal carbonate salts (e.g., $BaCO_3$, Ag_2CO_3) dissolve readily under acidic conditions. However, chelation of carbonate to $[(L)Co(III)]^{n+}$ centers (L = nta, trien, $(gly)_2$, $(NH_3)_4$, $(en)_2$, cyclen, *N*-mecyclen)[2] can lead to significant retardation of the rate of acid hydrolysis, with the rate constants for such reactions depending markedly on the identity of the ancillary ligand, L.[3] This is manifested most dramatically in the Co(III) complex cations $[Co(py)_4(O_2CO)]^+$,[4] $[Co([3^5]adz)(O_2CO)]^+$,[5]

† Dedicated to Emeritus Professor David A. Buckingham, an inspirational and exemplary practitioner of physical inorganic chemistry, on the happy occasion of his 70th birthday.

* To whom correspondence should be addressed. E-mail: blackman@alkali.otago.ac.nz. Fax: +64 3 479 7906.

(1) Palmer, D. A.; Van Eldik, R. *Chem. Rev* **1983**, *83*, 651−731.

(2) Abbreviations used are as follows: nta = nitrilotriacetic acid; cyclen = 1,4,7,10-tetraazacyclododecane; *N*-mecyclen = 1-Me-1,4,7,10-tetraazacyclododecane; adz = adamanzane; tpa = tris(2-pyridylmethyl)amine; pmea = bis(2-pyridylmethyl)-2-(2-pyridylethyl)amine; pmap = bis(2-(2-pyridyl)ethyl)(2-pyridylmethyl)amine; tepa = tris(2-pyridylethyl)amine.

(3) Buckingham, D. A.; Clark, C. R. *Inorg. Chem.* **1994**, *33*, 6171−9.

(4) Springborg, J.; Schäffer, C. E., *Acta Chem. Scand.* **1973**, *27*, 3312−22.

(5) Broge, L.; Søtofte, I.; Olsen, C. E.; Springborg, J. *Inorg. Chem.* **2001**, *40*, 3124−3129.

10.1021/ic0521325 CCC: $33.50 © 2006 American Chemical Society
Published on Web 02/17/2006

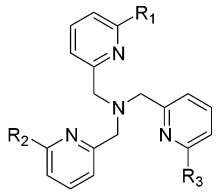

tpa: $R_1 = R_2 = R_3 = H$
Me-tpa: $R_1 = Me$, $R_2 = R_3 = H$
Me_2-tpa: $R_1 = R_2 = Me$, $R_3 = H$
Me_3-tpa: $R_1 = R_2 = R_3 = Me$

Figure 1. Structures of the tripodal tetraamine ligands.

and $[Co(pmap)(O_2CO)]^+$ [6] which show quite extraordinary stability in 12 M HCl, 25% HBr, and 6 M HCl, respectively, and the reasons for such unusual behavior are obviously of interest.

Our recent study of $[Co(L)(O_2CO)]^+$ complexes containing structurally similar pyridyl-based tripodal ancillary ligands (L = tpa, pmea, pmap, tepa) showed that these underwent acid hydrolysis significantly more slowly than complexes such as $[Co(NH_3)_4(O_2CO)]^+$ and $[Co(en)_2(O_2CO)]^+$, with the least reactive complex $[Co(pmap)(O_2CO)]^+$ showing little UV−vis spectral change in 6 M HCl over 4 hours.[6] Spectroscopic, ^{59}Co NMR, and X-ray structural data obtained for these complexes were consistent with the steric, rather than the electronic, features of the ancillary ligands being primarily responsible for the slow rates of hydrolysis; there was no correlation of hydrolysis rate with the electronic properties of the complexes, while the X-ray structural data showed that both the methylene protons and the proton at the 6-position of the pyridine rings within the tripodal ligands hindered protonation of the coordinated endo oxygen atoms of the carbonate ligand. We reasoned that replacement of these latter protons with more sterically demanding groups should retard the observed rate of acid hydrolysis even further, if sterics were indeed the important factor determining the rate of reaction. Of the four complexes studied, $[Co(tpa)(O_2CO)]^+$ was the most rapid to hydrolyze, and, as synthetic methods for derivatization of the tpa ligand at the 6 position are readily available,[7−9] the synthesis and study of Co(III) complexes of the methylated ligands Me-tpa, Me_2-tpa, and Me_3-tpa (Figure 1) could be readily achieved. In this paper, we show that the acid hydrolysis rates of these complexes are significantly slower than that of $[Co(tpa)(O_2CO)]^+$; we contend that this is further proof that the steric, rather than electronic, properties of the ancillary ligands primarily determine the rate of acid hydrolysis of the carbonate complexes and that protonation at an endo O atom is required for chelate ring opening to occur.

Experimental Section

General Methods. ^{1}H and ^{13}C NMR spectra were obtained in D_2O at 25.0 °C on a Varian VXR 300 MHz or Varian Europa 500 MHz spectrophotometer and were referenced to sodium 3-(trimethylsilyl)tetradeuteriopropionate (NaTSP, ^{1}H NMR) and either 2,2-dimethyl-2-silapentane-5-sulfonic acid sodium salt (DSS) or 1,4-dioxane (^{13}C NMR). ^{59}Co NMR spectra were recorded in D_2O on a Varian Europa 500 MHz spectrophotometer in a 10 mm NMR tube at 118.573 MHz, and chemical shifts are reported relative to an external reference of $K_3[Co(CN)_6]$ (0 ppm). Visible spectra were recorded in aqueous solution on a Varian Cary 500 Scan UV−vis NIR spectrophotometer. Kinetic data were recorded on the same instrument, thermostated at 25.0 °C. Comparative rate data for acid hydrolysis of $[Co(tpa)(O_2CO)]^+$, $[Co(Me\text{-}tpa)(O_2CO)]^+$, $[Co(Me_2\text{-}tpa)(O_2CO)]^+$, and $[Co(Me_3\text{-}tpa)(O_2CO)]^+$ under the same $[H_3O^+]$ were obtained at $[Co]_{total} = 1.0 \times 10^{-3}$ M and [HCl] = 6.0 M by monitoring the absorbance decrease at λ_{max} (487, 502, 516, and 544 nm for the tpa, Me-tpa, Me_2-tpa, and Me_3-tpa complexes, respectively), while rate data for the acid hydrolysis of $[Co(tpa)(O_2CO)]^+$ over the $[HClO_4]$ range of 0.10−1.00 M were obtained at $[Co]_{total} = 5.0 \times 10^{-3}$ M and $I = 1.0$ M ($NaClO_4$) ($\lambda = 487$ nm). Reactions were monitored to at least 95% completion, and data were fitted to a single exponential decay to obtain first-order rate constants (k_{obs}), reported values of which are averages of three concordant runs. Mass spectra were obtained on a Shimadzu LCMS-QP8000α system (mass range m/z 10−2000, resolution $R = 2$ M, 50% valley) using direct infusion via a manual Rheodyne injector (5 μL loop). Positive ionization techniques were used on an ESI probe (H_2O mobile phase, 0.2 mL min^{-1}, CDL temp 250 °C, 4.5 kV). Elemental analyses were performed by the Campbell Microanalytical Laboratory, University of Otago. Reported elemental percentages (C, H, N, Cl) are accurate to within ±0.4%.

Syntheses. All chemicals used were of LR grade or better. $Na_3[Co(O_2CO)_3]\cdot 3H_2O$,[10] $[Co(tpa)O_2CO]ClO_4\cdot H_2O$,[6] bis(2-pyridylmethyl)amine,[11] 2-formaldoximo-6-methylpyridine,[12] 6-methyl-2-aminomethylpyridine,[12] 2-(chloromethyl)-6-methylpyridine,[13] bis(2-pyridylmethyl)[(6-methyl-2-pyridyl)methyl]amine (Me-tpa),[7] 2-pyridylmethylbis(6-methyl-2-pyridylmethyl)amine (Me_2-tpa),[8] and tris-((6-methyl-2-pyridyl)methyl)amine (Me_3-tpa)[9] were prepared by literature methods. Conversion of Me-tpa, Me_2-tpa, and Me_3-tpa to the trihydrobromide salts was achieved by addition of excess HBr(aq) to the free base forms of the ligands, and removal of solvent (rotavap). Despite prolonged subsequent trituration with EtOH, the hydrobromide salts could only be isolated as oils. NMR assignments utilize the following labeling and numbering systems: py^A represents the two equivalent 6-methylpyridyl or pyridyl rings, while py^B represents the unique 6-methylpyridyl or pyridyl ring in the same plane as the carbonate ligand. The protons and carbon atoms of the pyridyl rings are numbered such that the carbon atom attached to the methylene carbon is C2.

CAUTION: Although no difficulties were experienced with the perchlorate complexes described herein, all perchlorate species should be treated as potentially explosive and handled with care.

$[Co(Me\text{-}tpa)(O_2CO)]ClO_4\cdot 0.5H_2O$ (Equatorial Isomer). Me-tpa·3HBr (12.05 g, 22.02 mmol) was added to a suspension of $Na_3[Co(O_2CO)_3]\cdot 3H_2O$ (8.97 g, 24.8 mmol) in H_2O (150 mL). The mixture was heated at 65 °C for 10 min and then filtered through Celite. The resulting red filtrate was diluted to ∼2.5 L and loaded onto a Sephadex SP C-25 cation-exchange column. Elution with 0.1 M $NaClO_4$(aq) removed a red band, which was concentrated

(6) Jaffray, P. M.; McClintock, L. F.; Baxter, K. E.; Blackman, A. G. *Inorg. Chem.* **2005**, *44*, 4215−4225.
(7) Zang, Y.; Kim, J.; Dong, Y.; Wilkinson, E. C.; Appelman, E. H.; Que, L., Jr. *J. Am. Chem. Soc.* **1997**, *119*, 4197−4205.
(8) Da Mota, M. M.; Rodgers, J.; Nelson, S. M. *J. Chem. Soc. A.* **1969**, 2036−44.
(9) Bebout, D. C.; Bush, J. F., II.; Crahan, K. K.; Bowers, E. V.; Butcher, R. J. *Inorg. Chem.* **2002**, *41*, 2529−36.
(10) Bauer, H. F.; Drinkard, W. C. *Inorg. Synth.* **1966**, *8*, 202−4.
(11) Højland, F.; Toftlund, H.; Yde Andersen, S. *Acta Chem. Scand.* **1983**, *A37*, 251−7.
(12) Fuentes, O.; Paudler, W. W. *J. Org. Chem.* **1975**, *40*, 1210−13.
(13) Jeromin, G. E.; Orth, W.; Rapp, B.; Weiss, W. *Chem. Ber.* **1987**, *120*, 649−51.

to low volume (rotavap). Red crystalline material deposited upon storage at 4 °C for 24 h. This material was filtered, washed with minimal volumes of ice cold water, and air-dried to yield the desired product as an isomeric mixture (4.51 g, 39%). A small portion of this product was recrystallized from the minimum volume of cold water to give X-ray quality crystals of isomerically pure equatorial [Co(Me-tpa)(O_2CO)]ClO_4·0.5H_2O. Anal. Calcd for $CoC_{20}H_{21}N_4O_{7.5}$Cl: C, 45.17; H, 3.98; N, 10.53; Cl, 6.66. Found: C, 45.30; H, 3.87; N, 10.52; Cl, 7.08. ESI-MS: calcd for $CoC_{20}H_{20}N_4O_3^+$ 423; found 423 [M^+], 408 [$M^+ - CH_3$], 303 [$M^+ - Co(CO_3)H$]. UV−vis (H_2O) [λ_{max}, nm, (ϵ, M^{-1} cm^{-1})]: 502 (154). ^{1}H NMR (D_2O): δ 8.75 (2H, dd, J = 6, 1 Hz, py^A-H_6), 8.12 (2H, td, J = 8, 1 Hz, py^A-H_4), 7.72 (2H, d, J = 8 Hz, py^A-H_5) 7.65 (3H, m, py^A-H_3 and $py^{B,Me}$-H_4), 7.32 (1H, d, J = 7 Hz, $py^{B,Me}$-H_5), 7.05 (1H, d, J = 8 Hz, $py^{B,Me}$-H_3), 5.26 (2H, d, J = 16 Hz, $py^{B,Me}$-CH_2), 5.06 (4H, m, py^A-CH_2), 3.17 (3H, s, py^B-CH_3). ^{13}C NMR (D_2O): δ 168.86 (1C, $py^{B,Me}$-C_2), 167.14 (1C, $py^{B,Me}$-C_6), 164.62 (2C, py^A-C_2), 153.63 (2C, py^A-C_6), 144.21 (2C, py^A-C_4), 142.68 (1C, $py^{B,Me}$-C_4), 130.64 (1C, $py^{B,Me}$-C_5), 129.34 (2C, py^A-C_5), 126.24 (2C, py^A-C_3), 121.45 (1C, $py^{B,Me}$-C_3), 71.96 (1C, $py^{B,Me}$-CH_2), 71.50 (2C, py^A-CH_2), 24.61 (1C, py^B-CH_3). The signal corresponding to the carbonate C atom could not be observed. ^{59}Co NMR (D_2O): δ 8606.

[Co(Me_2-tpa)(O_2CO)]ClO_4·0.5H_2O (Axial/Equatorial Isomer). Me_2-tpa·3HBr (1.30 g, 2.32 mmol) was added to a suspension of Na_3[Co(O_2CO)$_3$]·3H_2O (0.963 g, 2.66 mmol) in H_2O (18 mL). The mixture was heated at 65 °C for 10 min and filtered through Celite; the resulting pink filtrate was then diluted to 1 L and loaded onto a Sephadex SP C-25 cation-exchange column. Elution with 0.1 M $NaClO_4$(aq) removed a pink band that was concentrated to low volume (rotavap) to give a dark pink oil. This was triturated with 2-propanol (2 × 100 mL), with each 100 mL portion being stirred overnight. Most of the 2-propanol was decanted off, and the powder was then filtered off and redissolved in H_2O (∼50 mL); the solution was concentrated to low volume (rotavap) to give the product as a microcrystalline material (0.379 g, 30%). Pink crystals of sufficient quality for X-ray analysis were obtained upon slow cooling of a hot, concentrated aqueous solution to which $NaClO_4$(s) had been added. Anal. Calcd for $CoC_{21}H_{23}N_4O_{7.5}$Cl: C, 46.21; H, 4.25; N, 10.27; Cl, 6.49. Found: C, 45.86; H, 4.18; N, 10.16; Cl, 6.89. ESI-MS: calcd for $CoC_{21}H_{22}N_4O_3^+$ 437; found 437 [M^+], 422 [$M^+ - CH_3$], 317 [$M^+ - Co(CO_3)H$]. UV−vis (H_2O) [λ_{max}, nm, (ϵ, M^{-1} cm^{-1})]: 516 (227). ^{1}H NMR (D_2O): δ 8.65 (1H, d, J = 6 Hz, py-H_6), 8.04 (1H, t, J = 8 Hz, py^A-H_4), 7.95 (1H, t, J = 8 Hz, $py^{A,Me}$-H_4), 7.71 (1H, t, J = 8 Hz, $py^{B,Me}$-H_4), 7.62 (1H, t, J = 7 Hz, py^A-H_5), 7.55 (1H, d, J = 8 Hz, py^A-H_3), 7.53 (1H, d, J = 8 Hz, $py^{A,Me}$-H_3), 7.41 (1H, d, J = 8 Hz, $py^{B,Me}$-H_5), 7.35 (1H, d, J = 8 Hz, $py^{A,Me}$-H_5), 7.15 (1H, d, J = 8 Hz, $py^{B,Me}$-H_3), 5.48 (1H, d, J = 17 Hz), 5.25 (1H, d, J = 16 Hz), 5.12 (1H, d, J = 18 Hz), 4.97 (2H, m), 4.84 (1H, d, J = 19 Hz), 3.26 (3H, s, py^B−CH_3), 2.84 (3H, s, py^A−CH_3). ^{13}C NMR (D_2O): δ 168.27, 167.50, and 166.51 (3 × C_2), 164.16 and 163.75 ($py^{A,Me}$-C_6 and $py^{B,Me}$-C_6), 152.08 (py^A-C_6), 143.98, 143.79, and 142.57 (3 × C_4), 130.88, 130.40, and 129.02 (3 × C_5), 125.42, 123.69, and 122.13 (3 × C_3), 72.10, 71.44, and 71.28 (3 × CH_2), 25.02 (py^B-CH_3), 24.50 (py^A-CH_3). The signal corresponding to the carbonate C atom could not be observed. ^{59}Co NMR (D_2O): δ 9162.

[Co(Me_3-tpa)(O_2CO)]ClO_4. Me_3-tpa·3HBr (7.95 g, 13.8 mmol) was added to a suspension of Na_3[Co(O_2CO)$_3$]·3H_2O (11.29 g, 31.20 mmol) in H_2O (185 mL). The mixture was heated at 65 °C for 10 min and then filtered through Celite, and the resulting purple filtrate was diluted to 3 L and loaded onto a Sephadex SP C-25 cation-exchange column. Elution with 0.1 M $NaClO_4$(aq) removed a purple band, and purple crystals of sufficient quality for X-ray structural determination were deposited upon storage of this eluate at 4 °C for 12 h. The crystals were filtered, washed with minimal volumes of ice cold water and 2-propanol, and air-dried. The remaining eluate was reduced to low volume (rotavap) to give a further crop of microcrystalline [Co(Me_3-tpa)(O_2CO)]ClO_4 (2.33 g, 31%). Anal. Calcd for $CoC_{22}H_{24}N_4O_7$Cl: C, 47.97; H, 4.39; N, 10.17; Cl, 6.44. Found: C, 47.86; H, 4.40; N, 10.05; Cl, 6.82. ESI-MS: calcd for $CoC_{22}H_{24}N_4O_3^+$ 451; found 451 [M^+], 436 [$M^+ - CH_3$], 331 [$M^+ - Co(CO_3)H$]. UV−vis (H_2O) [λ_{max}, nm, (ϵ, M^{-1} cm^{-1})]: 544 (207). ^{1}H NMR (D_2O): δ 7.79 (2H, t, J = 8 Hz, $py^{A,Me}$-H_4), 7.70 (1H, t, J = 8 Hz, $py^{B,Me}$-H_4), 7.38 (1H, d, J = 8 Hz, $py^{B,Me}$-H_5), 7.36 (2H, d, J = 8 Hz, $py^{A,Me}$-H_3), 7.24 (2H, d, J = 8 Hz, $py^{A,Me}$-H_5), 7.18 (1H, d, J = 8 Hz, $py^{B,Me}$-H_3), 5.47 (2H, d, J = 16 Hz, $py^{B,Me}$-CH_2−), 4.93 (4H, m, $py^{A,Me}$-CH_2−), 3.45 (3H, s, py^B-CH_3), 2.90 (6H, s, py^A-CH_3). ^{13}C NMR (D_2O): δ 169.02 (1C, $py^{B,Me}$-C_6), 168.29 (2C, $py^{A,Me}$-C_6), 164.74 (2C, $py^{A,Me}$-C_2), 164.41 (1C, $py^{B,Me}$-C_2), 143.39 (2C, $py^{A,Me}$-C_4), 142.45 (1C, $py^{B,Me}$-C_4), 131.06 (2C, $py^{A,Me}$-C_5), 130.89 (1C, $py^{B,Me}$-C_5), 123.00 (2C, $py^{A,Me}$-C_3), 122.16 (1C, $py^{B,Me}$-C_3), 71.50 (2C, $py^{A,Me}$-CH_2), 71.47 (1C, $py^{B,Me}$-CH_2), 27.03 (1C, py^B-CH_3), 24.91 (2C, py^A-CH_3). The signal corresponding to the carbonate C atom could not be observed. ^{59}Co NMR (D_2O): δ 10251.

X-ray Crystallography. X-ray data were collected at 85 K on a Bruker Kappa APEX-II[14] system using graphite-monochromated Mo Kα radiation with exposures over 0.5°, and they were corrected for Lorentz and polarization effects using SAINT.[15] All structures were solved using SIR-97[16] running within the WinGX package,[17] and weighted full-matrix refinement on F^2 was carried out using SHELXL-97.[18] Hydrogen atoms attached to carbon and nitrogen were included in calculated positions and were refined as riding atoms with individual (or group, if appropriate) isotropic displacement parameters. Only water hydrogen atoms which could be found in the difference map were included in the final cycles of refinement. The two perchlorate ions in the asymmetric unit of [Co(Me_2-tpa)(O_2CO)]ClO_4·H_2O were badly disordered and were modeled as pairs of intersecting tetrahedra with the thermal ellipsoid of O24′ restrained to be approximately isotropic. Some disorder was also evident in the methyl groups of one of the two cations within the asymmetric unit. This was modeled as an approximately 72:28 distribution of the two possible dimethyl isomers having the methyl-substituted rings in a cis configuration. Two sets of disordered water molecules were found in the crystal structure of [Co(Me-tpa)(O_2CO)]ClO_4·4H_2O: O10 and O10a were disordered over two sites in an approximately 40:60 ratio, while O9, O9a, and O9b were disordered over three sites with a total occupancy of 2, giving individual occupancies of 0.88, 0.24, and 0.88, respectively. Similarly, two disordered water molecules were observed in the structure of [Co(tpa)(O_2CO)]ClO_4·2H_2O with occupancies for O36 and O36A (62:38) and O34 and O34A (70:30) being found.

Results and Discussion

Synthesis and Characterization of Carbonate Complexes. The new complexes [Co(Me-tpa)(O_2CO)]ClO_4·0.5H_2O, [Co(Me_2-tpa)(O_2CO)]ClO_4·0.5H_2O, and [Co(Me_3-

(14) *APEX-II*, version 1.0-27; Bruker AXS Inc.: Madison, WI, 2004.
(15) *SAINT*; Bruker AXS Inc.: Madison, WI, 2001.
(16) Altomare, A.; Burla, M. C.; Camalli, M.; Cascarano, G. L.; Giacovazzo, C.; Guagliardi, A.; Moliterni, A. G. G.; Polidori, G.; Spagna, R. *J. Appl. Crystallogr.* **1999**, *32*, 115−9.
(17) Farrugia, L. J. *J. Appl. Crystallogr.* **1999**, *32*, 837−38.
(18) Sheldrick, G. M.; Schneider, T. R. *Methods Enzymol.* **1997**, *277*, 319−43.

Table 1. UV−vis and ^{59}Co NMR Data for the Carbonate Complexes

complex	λ_{max} (nm)	ϵ (mol^{-1} L cm^{-1})	λ_{max} (nm)	ϵ (mol^{-1} L cm^{-1})	Δ (cm^{-1})	^{59}Co δ
$[Co(tpa)(O_2CO)]^+$	487	192	348	200	22 172	7965
$[Co(Me\text{-}tpa)(O_2CO)]^+$	502	154	355	126	21 562	8606
$[Co(Me_2\text{-}tpa)(O_2CO)]^+$	516	227	365	177	20 976	9162
$[Co(Me_3\text{-}tpa)(O_2CO)]^+$	544	207	379	236	19 970	10 251

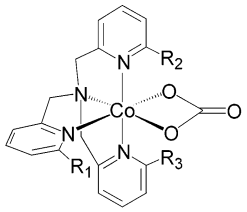

Me-tpa, equatorial isomer: R_1 = Me, R_2 = R_3 = H
Me-tpa, axial isomer: R_1 = R_3 = H, R_2 = Me
Me_2-tpa, axial-equatorial isomer: R_1 = R_2 = Me, R_3 = H
Me_2-tpa, axial-axial isomer: R_1 = H, R_2 = R_3 = Me

Figure 2. Possible geometric isomers of $[Co(Me\text{-}tpa)(O_2CO)]^+$ and $[Co(Me_2\text{-}tpa)(O_2CO)]^+$.

tpa)$(O_2CO)]ClO_4$ were prepared by reaction of the appropriate ligand trihydrobromide with an aqueous suspension of $Na_3[Co(O_2CO)_3]\cdot 3H_2O$ (slight excess) at 65 °C. Effervescence and a color change to red or purple was observed over 10 min, after which time the solution was cooled to room temperature, filtered, and purified on a Sephadex SP-C25 cation-exchange resin. The complexes were eluted with 0.1 M $NaClO_4$ and were crystallized as ClO_4^- salts. Partial desolvation of the mono- and dimethyl complexes occurs on air-drying, as shown by the differing molecular formulas of the crystallographic samples and those submitted for elemental analysis.

Geometric isomers of both the $[Co(Me\text{-}tpa)(O_2CO)]^+$ and $[Co(Me_2\text{-}tpa)(O_2CO)]^+$ cations are possible because of the different possible relative orientations of the methyl groups (Figure 2), and both NMR and X-ray crystallography were used to characterize the isomers obtained. The presence of two methyl signals in the ^{1}H NMR spectrum of crude $[Co(Me\text{-}tpa)(O_2CO)]^+$ was consistent with the presence of both the axial and equatorial isomers; however, crystallization of the crude material from cold water gave a single isomer. This was assigned as the equatorial isomer, in which the 6-methylpyridine ring lies in the same plane as the carbonate ligand, by analysis of ^{1}H and ^{13}C NMR spectra, and this assignment was subsequently confirmed by X-ray crystallographic analysis (see below). In contrast, NMR spectra of both crude and recrystallized $[Co(Me_2\text{-}tpa)(O_2CO)]ClO_4\cdot 0.5H_2O$ were consistent with the presence of only the equatorial-axial isomer, and this assignment was again confirmed by X-ray crystallography.

The four complexes exhibit remarkably different colors, ranging from orange $[Co(tpa)(O_2CO)]^+$ to purple $[Co(Me_3\text{-}tpa)(O_2CO)]^+$ (Figure 3), despite the fact that they have identical N_4O_2 donor atom sets and differ only in the number of methyl groups on the ancillary tripodal ligand. A similar, but less pronounced, gradation in colors was also observed for the $[Co(L)(O_2CO)]^+$ (L = tpa, pmea, pmap, tepa) series of complexes.[6] UV−vis spectroscopic data for the complexes are given in Table 1. The complexes all display two d−d

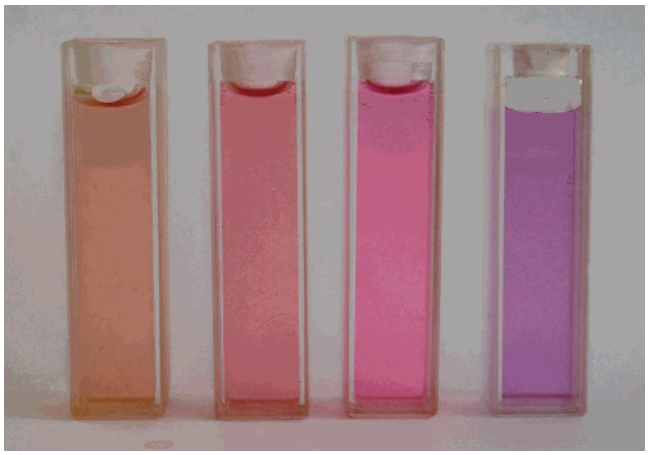

Figure 3. Solutions (2.0×10^{-3} M) of (from left) $[Co(tpa)(O_2CO)]^+$, $[Co(Me\text{-}tpa)(O_2CO)]^+$, $[Co(Me_2\text{-}tpa)(O_2CO)]^+$, and $[Co(Me_3\text{-}tpa)(O_2CO)]^+$ in water.

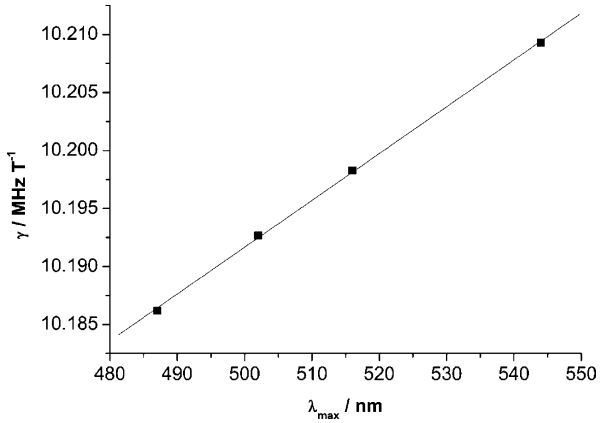

Figure 4. Plot of γ versus λ_{max} for the carbonate complexes.

transitions with those at shortest wavelength appearing as shoulders on an intense charge-transfer band. There is a progressive shift of the peak maxima to longer wavelengths as the number of methyl groups on the ancillary ligand increases, and there is also a significant concomitant broadening of the low-energy band. The data in Table 1 confirm that the ligand field strengths of the four tripodal ligands decrease as the number of methyl groups increase, with a difference of 2202 cm^{-1} in the value of Δ between $[Co(tpa)(O_2CO)]^+$ and $[Co(Me_3\text{-}tpa)(O_2CO)]^+$.[19] This variation in ligand field strength can be rationalized by investigation of the X-ray structures of the four complexes. The average Co−N bond distance increases significantly (1.915, 1.936, 1.950, and 1.982 Å for the tpa, Me-tpa, Me_2-tpa, and Me_3-tpa complexes, respectively) as the ligands become more sterically demanding because of the unfavorable steric

(19) Δ values were calculated as described in ref 22, assuming $C = 4B$.

Table 2. Crystal Data and Structure Refinement for the Co(III) Carbonate Chelates

	[Co(tpa)(O_2CO)]ClO_4·2H_2O	[Co(Me-tpa)(O_2CO)]ClO_4·4H_2O	[Co(Me_2-tpa)(O_2CO)]ClO_4·H_2O	[Co(Me_3-tpa)(O_2CO)]ClO_4
empirical formula	$C_{19}H_{22}ClCoN_4O_9$[a]	$C_{20}H_{28}ClCoN_4O_{11}$ [a]	$C_{21}H_{24}ClCoN_4O_8$[b]	$C_{22}H_{24}ClCoN_4O_7$
fw	544.79	594.84	554.82	550.83
T (K)	85(2)	85(2)	85(2)	85(2)
λ (Å)	0.71069	0.71069	0.71069	0.71069
space group	$P\bar{1}$	$P\bar{1}$	$P2_1/c$	$P\bar{1}$
a (Å)	16.230(5)	8.252(5)	23.000(5)	8.065(5)
b (Å)	17.229(5)	9.846(5)	12.792(5)	13.630(5)
c (Å)	17.339(5)	15.243(5)	15.931(5)	21.909(5)
α (deg)	106.760(5)	78.662(5)		79.876(5)
β (deg)	92.809(5)	80.160(5)	102.896(5)	80.864(5)
γ (deg)	108.004(5)	84.412(5)		79.566(5)
V (Å^3)	4364(2)	1193.8(10)	4569(2)	2311.5(17)
Z	8	2	8	4
D_c (Mg m^{-3})	1.651	1.638	1.607	1.583
μ (mm^{-1})	0.970	0.899	0.925	0.911
Final R indices	R1 = 0.0349	R1 = 0.0361	R1 = 0.0717	R1 = 0.0292
[$I > 2\sigma(I)$]	wR2 = 0.0799	wR2 = 0.0936	wR2 = 0.1537	wR2 = 0.0809
R indices	R1 = 0.0451	R1 = 0.0412	R1 = 0.0820	R1 = 0.0336
(all data)	wR2 = 0.0864	wR2 = 0.0968	wR2 = 0.1582	wR2 = 0.0866

[a] Some water hydrogen atoms not located. [b] No water hydrogen atoms located.

Table 3. Selected Bond Lengths (Å) and Angles (deg) for the Co(III) Carbonate Chelates[a]

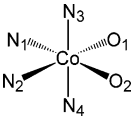

complex	Co−O1	Co−O2	Co−N1	Co−N2	Co−N3	Co−N4	N1−Co−O1	N2−Co−O2
[Co(tpa)(O_2CO)]$^{+b}$	1.9078(18)	1.8966(18)	1.938(2)	1.892(2)	1.907(2)	1.912(2)	101.42(8)	101.89(9)
[Co(tpa)(O_2CO)]$^+$	1.8994(18)	1.8867(19)	1.943(2)	1.900(2)	1.916(2)	1.911(2)	101.37(9)	101.62(9)
[Co(tpa)(O_2CO)]$^+$	1.8952(18)	1.9081(18)	1.930(2)	1.898(2)	1.906(2)	1.911(2)	99.29(9)	104.06(8)
[Co(tpa)(O_2CO)]$^+$	1.9045(18)	1.8962(18)	1.938(2)	1.901(2)	1.921(2)	1.912(2)	100.79(9)	102.70(9)
[Co(Me-tpa)(O_2CO]$^+$	1.8853(12)	1.9262(15)	1.9345(16)	1.9673(15)[d]	1.9184(17)	1.9232(17)	94.64(6)	109.12(6)
[Co(Me_2-tpa)(O_2CO)]$^{+c}$	1.897(3)	1.916(3)	1.930(4)	1.976(4)[d]	1.930(4)	1.955(4)[d]	96.69(17)	108.18(15)
[Co(Me_2-tpa)(O_2CO)]$^+$	1.877(3)	1.914(3)	1.944(4)	1.966(4)[d]	1.974(4)[d]	1.923(4)	95.84(17)	107.93(16)
[Co(Me_3tpa)(O_2CO)]$^{+c}$	1.8833(10)	1.9213(15)	1.9355(15)	1.9850(12)[d]	1.9791(12)[d]	2.0287(12)[d]	94.35(5)	109.67(4)
[Co(Me_3tpa)(O_2CO)]$^+$	1.8863(11)	1.9149(15)	1.9341(16)	2.0016(13)[d]	2.0150(12)[d]	1.9755(12)[d]	95.97(5)	108.89(4)

[a] The atom numbering scheme is given in the diagram. N1 corresponds to the aliphatic tertiary N atom of the tripodal ligand in all cases. [b] Four independent molecules in the asymmetric unit. [c] Two independent molecules in the asymmetric unit. [d] Co−N bond to a methylated pyridine ring.

interactions between the methyl groups and the carbonate ligand and also those between the methyl groups themselves in the di- and trimethyl complexes. Such an increase in the Co−N bond length leads logically to a decrease in the magnitude of the d-orbital splitting through poorer M−L orbital overlap.

The ^{59}Co NMR data given in Table 1 also attest to the different ligand field strengths exerted by the tripodal ligands with a chemical shift range of over 2000 ppm observed across the series of complexes, reflecting a decrease in electron density at the Co nucleus as the number of methyl groups increases. The expected linear relationship between λ_{max} and γ [20,21] is observed (Figure 4), but the y intercept of (9.900 ± 0.003) MHz T^{-1}, which should correspond to γ_o(^{59}Co), the magnetogyric ratio of the bare Co nucleus, differs from values obtained previously from more highly symmetrical complexes (10.04−10.05 MHz T^{-1}). The reasons for this discrepancy have been remarked upon previously.[22]

X-ray Crystallography. X-ray collection and refinement data for the four complexes are given in Table 2, while selected bond lengths and angles are given in Table 3 and diagrams of the complex cations are given in Figure 5. Our previously reported structure of [Co(tpa)(O_2CO)]ClO_4·H_2O [6] at 168 K exhibited poor R_{int}, R_σ, and final R factors and this prompted us to recollect a dataset at lower temperature (85 K) and reinvestigate the X-ray structure of this complex. In so doing, we obtained much better data, as shown by the significantly better R_{int} and R_σ values, and the final R factor (R1 = 3.49%) was much lower than that obtained in our original solution (R1 = 11.58%). Both solutions were obtained in the same space group ($P\bar{1}$) but differed in Z, the 85 K structure having $Z = 8$, whereas previously we obtained $Z = 4$ at 168 K. It may be that the complex undergoes a phase change between these two temperatures or that our original structure was in fact in error. Nevertheless, the 85 K structure displays lower esd values, and we shall use bond lengths and angles obtained from these data in our subsequent discussions.

In all cases, the structures consist of a central Co(III) ion coordinated to all four N atoms of the tripodal amine ligand

(20) Griffith, J. S.; Orgel, L. E. *Trans. Faraday Soc.* **1957**, *53*, 601−6.
(21) Freeman, R.; Murray, G. R.; Richards, R. E. *Proc. R. Soc. London* **1957**, *A242*, 455−66.
(22) Bramley, R.; Brorson, M.; Sargeson, A. M.; Schaeffer, C. E. *J. Am. Chem. Soc.* **1985**, *107*, 2780−7.

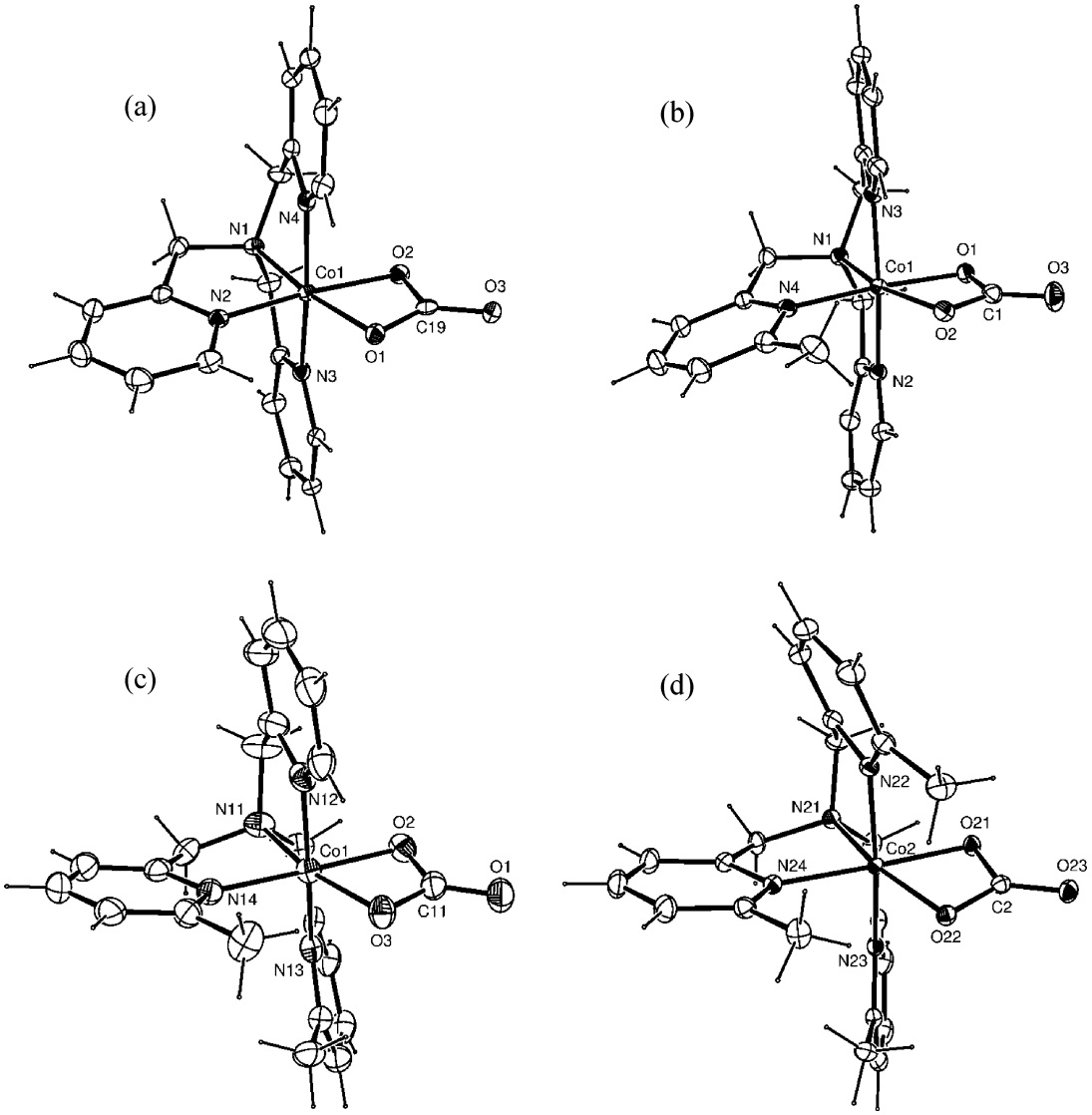

Figure 5. ORTEP diagrams of the (a) $[Co(tpa)(O_2CO)]^+$, (b) $[Co(Me\text{-}tpa)(O_2CO)]^+$, (c) $[Co(Me_2\text{-}tpa)(O_2CO)]^+$, and (d) $[Co(Me_3\text{-}tpa)(O_2CO)]^+$ cations. Thermal ellipsoids are drawn at the 50% probability level.

and two O atoms of the chelated carbonate ligand. The introduction of methyl substituents at the 6-position of the pyridine rings has significant structural ramifications. As alluded to above, the average Co−N bond lengths increase by 0.067 Å across the four complexes, with those for the tpa complex being the shortest. Interestingly, the Co−N bond to the tertiary N atom of the tripodal ligand remains relatively constant in length across the series; while it is the longest Co−N bond in $[Co(tpa)(O_2CO)]^+$, it is the shortest in $[Co(Me_3\text{-}tpa)(O_2CO)]^+$. The significant steric effects imparted by the methyl groups in $[Co(Me\text{-}tpa)(O_2CO)]^+$ and $[Co(Me_2\text{-}tpa)(O_2CO)]^+$ are shown by the fact that the Co−N bonds to the methylated pyridine rings are substantially longer than those to the unsubstituted pyridine rings in both complexes, which suggests that the lengthening of the former helps minimize destabilizing interactions involving the methyl groups. The Co−O bond lengths are relatively unaffected by the changing nature of the tripodal ligand, but it can be seen that introduction of a 6-methyl substituent on the equatorial pyridyl ring lengthens the adjacent Co−O bond very slightly relative to that in $[Co(tpa)(O_2CO)]^+$. Similar trends in M−L bond lengths have been observed in the structurally characterized complexes $[Fe(tpa)(MeCN)_2](BPh_4)_2$[23] and $[Fe(Me_3\text{-}tpa)(MeCN)_2](BPh_4)_2$,[7] where the average Fe−N distance increases from 1.965 Å in the former to 2.197 Å in the latter.

Crystallographic analysis of $[Co(Me\text{-}tpa)(O_2CO)]ClO_4\cdot 4H_2O$ and $[Co(Me_2\text{-}tpa)(O_2CO)]ClO_4\cdot 0.5H_2O$ confirms that they are the equatorial and equatorial-axial isomers, respectively. The inherent strain present in the $[Co(Me\text{-}tpa)(O_2CO)]^+$ cation is manifested by the orientation of the 6-methylpyridine ring. Whereas the equatorial pyridine ring is essentially coplanar with the carbonate ligand in all four unique $[Co(tpa)(O_2CO)]^+$ cations, there is an angle of 17.95° between the mean planes of the 6-methylpyridine ring and the carbonate ligand in the $[Co(Me\text{-}tpa)(O_2CO)]^+$ cation (Figure 5b). Similarly, while the mean planes of the axial rings deviate from coplanarity by a maximum of 5.79° in the $[Co(tpa)(O_2CO)]^+$ cations, the corresponding angle in the $[Co(Me\text{-}tpa)(O_2CO)]^+$ cation is 13.33°. The introduction

(23) Diebold, A.; Hagen, K. S. *Inorg. Chem.* **1998**, *37*, 215−23.

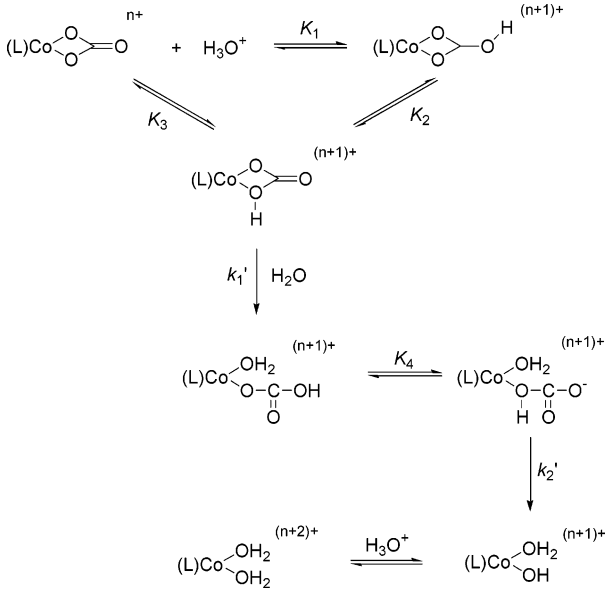

Figure 6. Mechanism of hydrolysis of $[(L)Co(O_2CO)]^{n+}$ complexes.

of additional 6-methylpyridyl rings leads to still more distortion within the coordinated tripodal ligands with the angle between the axial ring mean planes reaching 35.55° in one of the two independent $[Co(Me_3\text{-tpa})(O_2CO)]^+$ cations, and this is particularly clear in Figure 5d. The O−Co−O angles are relatively constant across the four complexes (69.2 ± 0.4°), as are the N−Co−N angles trans to these (86.7 ± 0.8°). However, the two N−Co−O angles in the equatorial plane undergo significant change as 6-methylpyridyl rings are introduced. The N2−Co−O2 bond angle expands from ∼102° in $[Co(tpa)(O_2CO)]^+$ to ∼109° in the methylated complexes, presumably to minimize steric interaction of the equatorial methyl group with O2 of the chelated carbonate ligand, with a concomitant reduction in the trans N1−Co−O1 angle from ∼101 to ∼95°. Again, similar trends are seen in $[Fe(tpa)(MeCN)_2](BPh_4)_2$ and $[Fe(Me_3\text{-tpa})(MeCN)_2](BPh_4)_2$.

Kinetics of Acid Hydrolysis. The mechanism of acid hydrolysis of the $[(L)Co(O_2CO)]^{n+}$ complexes, as elucidated by Buckingham and Clark,[3] is shown in Figure 6, and it involves initial protonation of the carbonate ligand prior to the rate-determining Co−O cleavage and ring opening. In contrast to free carbonate, chelated carbonate contains two types of inequivalent oxygen atoms[24] and hence two possible sites of protonation, the coordinated endo oxygens and the exo oxygen. However, only protonation at an endo oxygen atom is proposed to lead to reaction. While it is essentially impossible to measure the equilibrium constant for protonation solely at either endo oxygen (K_3), analysis of kinetic data allows an estimate of the observed protonation constant K ($= K_1 + K_3$) to be made, and a comparison of this value with those obtained for other complexes may give an indication of the extent of protonation at the endo O atom, assuming that protonation at the unhindered exo O atom remains relatively unaffected upon changing the ancillary ligand.

(24) Depending on the symmetry of the ancillary ligand(s), all three oxygen atoms of a chelated carbonate ligand can be inequivalent.

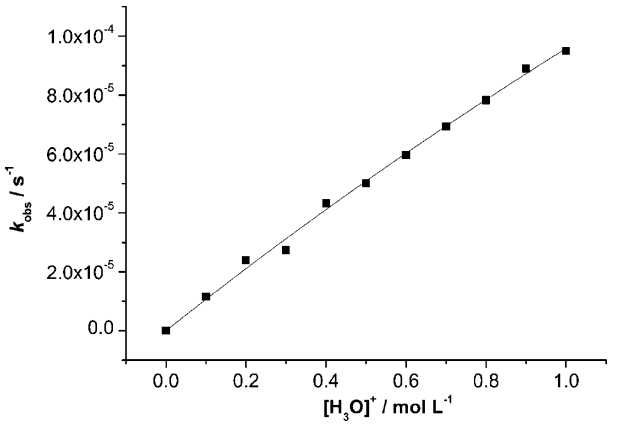

Figure 7. Rate data for the acid hydrolysis of $[Co(tpa)(O_2CO)]^+$. $[Co]_T = 5.0 \times 10^{-3}$ M, $I = 1.0$ M ($NaClO_4$), 25.0 °C.

Figure 7 shows a plot of k_{obs} versus $[H_3O^+]$ for the acid hydrolysis of $[Co(tpa)(O_2CO)]^+$ over the $[H_3O^+]$ range of 0.10−1.0 M at 25.0 °C. In contrast to the analogous plots for other, more reactive, complexes, the plot in Figure 7 shows only very slight curvature. This is consistent with a preequilibrium involving protonation of the chelated carbonate ligand, but, in contrast to other complexes studied previously,[3] such protonation is far from complete at $[H_3O^+] = 1.0$ M. Fitting of these data to the rate expression

$$k_{obs} = \frac{kK[H_3O^+]}{1 + K[H_3O^+]}$$

gives $K = 0.13\ M^{-1}$ and $k = 8.4 \times 10^{-4}\ s^{-1}$, where $K = K_1 + K_3$ and $k = K_2k_1'$ (Figure 6). These data show that the value of k for $[Co(tpa)(O_2CO)]^+$ is at least an order of magnitude less than that for $[Co(N\text{-mecyclen})(O_2CO)]^+$, the least reactive complex studied by Buckingham and Clark. Assuming that k_1' remains relatively constant over the complexes studied, the rate difference then resides in the value of K_2 and thus in the ability of the complex protonated on the exo O atom to transfer a proton to the endo O atom. Obviously the steric bulk of the tpa ligand impedes such transfer and this results in the relatively slow observed Co−O cleavage. Similarly, the value of K for $[Co(tpa)(O_2CO)]^+$ is somewhat smaller than those found in other complexes ($0.44-1.8\ M^{-1}$) [3], and this can be attributed, at least in part, to a smaller value of K_3, the equilibrium constant for direct protonation at the endo O atom.

Rate data for the three methylated complexes could not easily be obtained under the same conditions used for $[Co(tpa)(O_2CO)]^+$ because of both solubility problems and the slowness of the reactions (a solution of $[Co(Me_2\text{-tpa})(O_2CO)]^+$ in 1.0 M $HClO_4$ displayed a strictly linear absorbance decrease over 17 h). It was thus more convenient to obtain comparative rate data for the four complexes at [HCl] = 6.0 M, and these are given in Table 4. It is obvious from these data that increasing the steric bulk of the tripodal ligand has a significant retarding effect on the rate of acid hydrolysis. Introduction of a single equatorial 6-methylpyridyl ring slows the observed rate by a factor of 25, while both the di- and trimethyl complexes react approximately 90 and 50 times

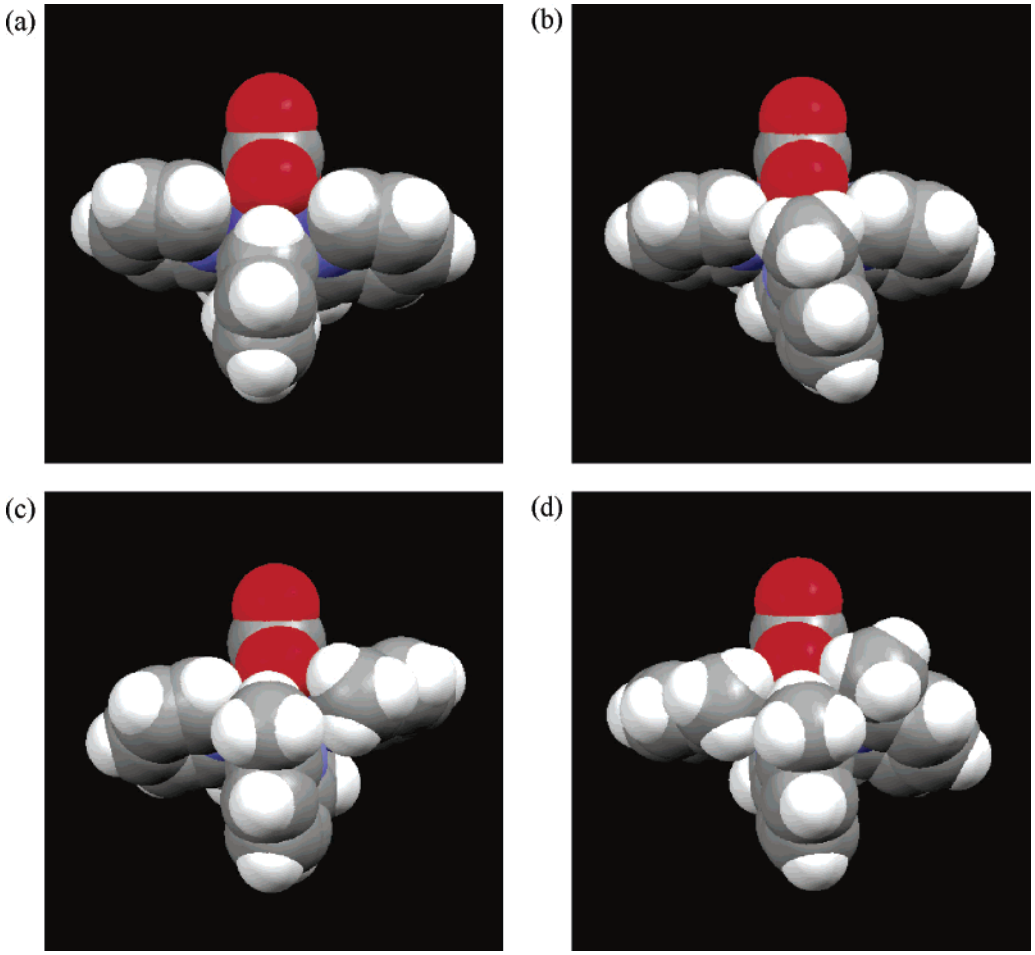

Figure 8. Space filling diagrams of (a) $[Co(tpa)(O_2CO)]^+$, (b) $[Co(Me\text{-}tpa)(O_2CO)]^+$, (c) $[Co(Me_2\text{-}tpa)(O_2CO)]^+$, and (d) $[Co(Me_3\text{-}tpa)(O_2CO)]^+$. Oxygen atoms of the carbonate ligand are red.

Table 4. Rate Data for the Acid Hydrolysis of $[Co(tpa)(O_2CO)]^+$, $[Co(Me\text{-}tpa)(O_2CO)]^+$, $[Co(Me_2\text{-}tpa)(O_2CO)]^+$, and $[Co(Me_3\text{-}tpa)(O_2CO)]^+$ at 25.0 °C[a]

complex	k_{obs} (s^{-1})	$t_{1/2}$ (min)
$[Co(tpa)(O_2CO)]^+$	1.79×10^{-3}	6.45
$[Co(Me\text{-}tpa)(O_2CO)]^+$	7.14×10^{-5}	162
$[Co(Me_2\text{-}tpa)(O_2CO)]^+$	2.02×10^{-5}	572
$[Co(Me_3\text{-}tpa)(O_2CO)]^+$	3.73×10^{-5}	310

[a] $[HCl] = 6.0$ M, $[Co]_{Total} = 1.0 \times 10^{-3}$ M.

more slowly than $[Co(tpa)(O_2CO)]^+$, respectively, under the same conditions. Electronically, tpa and Me_3-tpa are similar, with the three protonation constants of Me_3-tpa being slightly greater than those for tpa. Despite this, the respective formation constants for reaction of these ligands with a number of divalent transition metal ions are very different, with the Me_3-tpa species being significantly *less* stable in all cases,[25] and this behavior has been attributed to steric factors. Similarly, we contend that steric factors are responsible for the observed rate differences in the acid hydrolysis of the $[Co(L)(O_2CO)]^+$ complexes. Inspection of the space-filling diagrams in Figure 8 shows that one of the endo oxygen atoms is significantly sterically hindered by the adjacent equatorial methyl group in $[Co(Me\text{-}tpa)(O_2CO)]^+$ relative to $[Co(tpa)(O_2CO)]^+$, and this hindrance increases further with the introduction of axial methyl groups in $[Co(Me_2\text{-}tpa)(O_2CO)]^+$ and $[Co(Me_3\text{-}tpa)(O_2CO)]^+$. Protonation of this endo oxygen atom, whether it be directly from bulk solvent or via proton transfer from the exo oxygen atom, thus becomes more difficult, leading to a decrease in the observed hydrolysis rate. Our results are also consistent with the endo, rather than the exo, O atom as being the mechanistically important site of protonation as it is only the endo O atoms that are affected by the increasing steric bulk of the tripodal amine ligand. Figure 8 shows that the exo O atom in each complex remains similarly accessible to protonation regardless of the nature of the ancillary ligand, and thus protonation at this site is unlikely to be responsible for the observed rate differences in chelate ring opening. This is in accordance with the fact that some chelated bicarbonate complexes protonated at the exo oxygen have significant stability and can be isolated.[5,6,26] $[Co(Me_3\text{-}tpa)(O_2CO)]^+$ reacts more rapidly than $[Co(Me_2\text{-}tpa)(O_2CO)]^+$ despite the fact that the endo oxygen in the trimethyl complex appears to be more sterically hindered than that in the dimethyl complex, and the reason for this order of reactivity is not immediately obvious. However, it may be that the activation

(25) Anderegg, G.; Hubmann, E.; Podder, N. G.; Wenk, F. *Helv. Chim. Acta* **1977**, *60*, 123−40.

(26) Baxter, K. E.; Hanton, L. R.; Simpson, J.; Vincent, B. R.; Blackman, A. G. *Inorg. Chem.* **1995**, *34*, 2795−6.

energy for chelate ring opening of the endo-protonated species is lower for the trimethyl complex because of the greater relief of steric strain that occurs on hydrolysis. The X-ray structural data (Figures 5c and 5d) are in agreement with such a proposal. It is also interesting to note that acid hydrolysis of both $[Co(Me_2\text{-tpa})(O_2CO)]^+$ and $[Co(Me_3\text{-tpa})(O_2CO)]^+$ gives Co(II) species as the final products, in contrast to $[Co(tpa)(O_2CO)]^+$ and $[Co(Me\text{-tpa})(O_2CO)]^+$ which give $[Co(L)(OH_2)_2]^{3+}$. A similar reduction to Co(II) was observed upon acid hydrolysis of $[Co(tepa)(O_2CO)]^+$.[6]

Previous studies have also found significant structural and reactivity differences between complexes containing tpa and methylated tpa ligands. For example, $[Fe(tpa)(MeCN)_2]^{2+}$ is low-spin, but $[Fe(Me\text{-tpa})(MeCN)_2]^{2+}$, $[Fe(Me_2\text{-tpa})(MeCN)_2]^{2+}$, and $[Fe(Me_3\text{-tpa})(MeCN)_2]^{2+}$ are all high-spin. This observation is consistent with the results presented above, as the tripodal ligands exert a progressively weaker ligand field across the series tpa → Me_3-tpa, which lessens the magnitude of the d-orbital splitting and allows access to high-spin Fe(II). The longer Fe−N bonds in the complexes containing the methylated ligands are also better accommodated by the larger high-spin Fe(II) ion.[7] Likewise, redox potentials for the Cu complexes, $[Cu(L)(OH_2)]^{2+}$ (L = tpa, Me-tpa, Me_2-tpa, Me_3-tpa), become progressively more positive as the number of methyl groups increases,[27] while the Cu(I) complexes containing these ligands display markedly different reactivities toward dioxygen.[28−31] In all cases, the reactivity differences appear to be the result of the steric effects of the methyl groups of the tripodal ligand and the structural consequences of these.

Conclusions. It can be seen from this work that increasing the steric bulk of the ancillary ligand in complexes containing chelated carbonate can lead to significant increases in the stability of these complexes in acidic aqueous solution. Such an observation could conceivably be used to advantage in the synthesis of model complexes for carbonic anhydrase, in which a Zn^{2+}-chelated bicarbonate species is thought to be an important intermediate in the biological hydration of CO_2.[32,33] Similarly, the correct choice of a sterically hindered ancillary ligand may prove crucial in stabilizing the Co(III) complexes containing usually labile ligands such as ClO_4^- and $CF_3SO_3^-$ in aqueous solution. Our studies in these areas are ongoing.

Acknowledgment. L.F.M. thanks the Foundation for Research, Science and Technology for the award of a Bright Futures Scholarship. This work was supported by the Department of Chemistry, University of Otago.

Supporting Information Available: Crystallographic data (CIF) for the structures described herein. This material is available free of charge via the Internet at http://pubs.acs.org.

IC0521325

(27) Nagao, H.; Komeda, N.; Mukaida, M.; Suzuki, M.; Tanaka, K. *Inorg. Chem.* **1996**, *35*, 6809−15.
(28) Jacobson, R. R.; Tyeklar, Z.; Farooq, A.; Karlin, K. D.; Liu, S.; Zubieta, J. *J. Am. Chem. Soc.* **1988**, *110*, 3690−2.
(29) Uozumi, K.; Hayashi, Y.; Suzuki, M.; Uehara, A. *Chem. Lett.* **1993**, 963−6.
(30) Hayashi, H.; Fujinami, S.; Nagatomo, S.; Ogo, S.; Suzuki, M.; Uehara, A.; Watanabe, Y.; Kitagawa, T. *J. Am. Chem. Soc.* **2000**, *122*, 2124−5.
(31) Hayashi, H.; Uozumi, K.; Fujinami, S.; Nagatomo, S.; Shiren, K.; Furutachi, H.; Suzuki, M.; Uehara, A.; Kitagawa, T. *Chem. Lett.* **2002**, 416−7.
(32) Bottoni, A.; Lanza, C. Z.; Miscione, G. P.; Spinelli, D. *J. Am. Chem. Soc.* **2004**, *126*, 1542−50.
(33) Acharya, A. N.; Das, A.; Dash, A. C. *Adv. Inorg. Chem.* **2004**, *55*, 127−99.